ISSN 1606-867X (Print)
ISSN 2687-0711 (Online)
Condensed Matter and Interphases
Kondensirovannye Sredy i Mezhfaznye Granitsy
https://journals.vsu.ru/kcmf/

Original articles

Research article
https://doi.org/10.17308/kcmf.2025.27/12810

Diffractometric studies of the PA MBE grown of GaN layers on silicon substrates without their nitridation and an intermediate AlN nucleation layers

P. V. Seredin[1]✉, O. K. Kosheleva[1], D. L. Goloshchapov[1], N. S. Builov [1], Ya. A. Peshkov[1], A. M. Mizerov[2], S. N. Timoshnev[2], M. S. Sobolev[2], Sh. Sh. Sharofidinov[3]

*[1]Voronezh State University,
Universitetskaya pl. 1, Voronezh 394018, Russian Federation*

*[2]Alferov University,
8 ul. Khlopina, Bld. 3, letter A, Saint Petersburg 194021, Russian Federation*

*[3]Ioffe Physical Technical Institute, Russian Academy of Sciences,
26 Politekhnicheskaya st., Saint Petersburg 194021, Russian Federation*

Abstract

Purpose: The paper describes structural features of the growth of GaN layers synthesized by plasma-assisted molecular beam epitaxy on silicon substrates without substrate nitridation and without the formation of an aluminum-containing interlayer.

Experimental: High-resolution X-ray diffractometry was used to show that the proposed method can be used to grow strain-free GaN films.

It was found that in GaN layers grown directly on the Si substrate after its surface passivation by Ga atoms, the value of residual strain was at 300 MPa, while the use of indium atoms as a surfactant during the growth of the GaN layer resulted in a higher residual strain.

Conclusions: The obtained results are important for understanding the viability of the proposed approach for the formation of GaN layers directly integrated with Si without substrate nitridation and the formation of an aluminum-containing buffer. This method opens new opportunities for designing AIIIN-based optoelectronic devices.

Keywords: Plasma-assisted molecular beam epitaxy, GaN layers, Silicon substrate, X-ray diffraction, Strain-free GaN films

Funding: The study was carried out within the framework of the grant of the Ministry of Education and Science of the Russian Federation (project No. FZGU-2023-0006). PA MBE synthesis of the samples was carried out as a part of the grant provided by the Ministry of Science and Higher Education of the Russian Federation (grant No. FSRM-2023-0006).

Acknowledgements: The research was carried out using the equipment of the Laboratory of Gallium Nitride and Silicon Electronics of Voronezh State University and the Research Institute of Electronic Technology.

For citation: Seredin P. V., Kosheleva O. K., Goloshchapov D. L., Buylov N. S., Peshkov Y. A., Mizerov A. M., Timoshnev S. N., Sobolev M. S., Sharofidinov Sh. Sh. Diffractometric studies of the PA MBE grown of GaN layers on silicon substrates without their nitridation and an intermediate AlN nucleation layer. *Condensed Matter and Interphases*. 2025;27(2): 308–315. https://doi.org/10.17308/kcmf.2025.27/12810

Для цитирования: Середин П. В., Кошелева О. К., Голощапов Д. Л., Буйлов Н. С., Пешков А. Я., Мизеров А. М., Тимошнев С. Н., Соболев М. С., Шарофидинов Ш. Ш. Дифрактометрические исследования особенностей формирования слоев GaN на подложках кремния методом МПЭ ПА без использования процедуры нитридизации подложки и промежуточного AlN зародышевого слоя. *Конденсированные среды и межфазные границы*. 2025;27(2): 000-000. https://doi.org/10.17308/kcmf.2025.27/12810

✉ Pavel V. Seredin, e-mail: paul@phys.vsu.ru

1. Introduction

AIIIN semiconductors, with GaN being the most prominent example, have excellent electrophysical and optical properties that make them ideal for their use in high-power, high-frequency electronic devices [1,2]. However, there are still some unresolved problems related to the growth of high quality AIIIN layers on silicon substrates, which are most affordable for the production of microelectronic devices. These problems are associated with significant differences in the parameters of crystal lattices and thermal expansion coefficients [3].

Over the past decades, many methods have been proposed to reduce number of defects in the operating area [4, 5], with the most prominent of them being the use of Al transition and buffer layers. However, methods for optimizing AIIIN growth conditions vary depending on the used substrate. Interestingly, several studies have demonstrated that optical and electronic devices can be manufactured without intermediate layers like AlN or AlGaN.

In our previous work concerned with the study of the initial stages of plasma-assisted molecular beam epitaxy (PA MBE) of GaN layers on Si(111) substrates, it was demonstrated that the smoothest surfaces of GaN layers on Si(111) substrates can be obtained either without pre-epitaxial substrate nitridation or after high-temperature nitridation (TN = 850 °C) [6]. Therefore, it is extremely important to study the mechanisms of nitride growth in the region of the epitaxial layer/substrate hetero-interface, which would effectively reduce the elastic stresses to a level where microcracks and defects are not formed in the operating area. Thus, this paper describes the results of diffractometric studies of the peculiarities of PA MBE growth of GaN layers on silicon substrates without substrate nitridation and the formation of an intermediate AlN nucleation layer under Ga-enriched conditions and with additional In flow intended in order to increase the surface mobility of adatoms.

2. Materials and methods

In the study, the GaN epitaxial layers were grown by PA MBE technique on a Veeco Gen 200 setup, which allows simultaneously using up to 4 four-inch plates (or one substrate with a diameter of up to 200 mm) during the growth process [6]. Undoped GaN layers were grown on semi-insulating Si(111) substrates ($R > 10{,}000$ Ohm/cm) that had been treated using the Shiraki method.

The PA MBE synthesis of GaN layers consisted of two stages. First, a low-temperature LT-GaN nucleation layer with a thickness of ~10 nm was grown. Then (second stage), the main GaN layer was grown, which for A-type samples was synthesized at Tp = 720 °C, while for B-type samples, the main GaN layer was under a similar nitrogen flow, but at a lower temperature of Tp = 700 °C, with the addition of indium flow intended to increase the surface mobility of the adatoms and consequently achieve a smoother GaN surface.

Reflection high-energy electron diffraction (RHEED) was used for in-situ observation of the nucleation and changes in the surface morphology of the GaN/Si(111) layers. It was found that the onset of the growth was accompanied by a decrease in the intensity of the initial RHEED pattern of the substrate followed by the formation of misoriented LT-GaN grains (“polycrystalline” RHEED pattern) characteristic of nucleation. At the beginning of the main GaN layer growth, there was a gradual formation of a “dot” RHEED pattern, characteristic of the growth of a continuous layer with a developed surface morphology. Further growth of the main GaN layer was accompanied by a transition from a “dot” to “linear” RHEED pattern, indicating a transition from nanocolumnar to two-dimensional growth.

Fig. 1 schematically shows the technological profiles of the grown samples.

High-resolution X-ray diffraction data were obtained at 305 K using a DRON-8T diffractometer. The 2θ-ω scans and ω rocking curves (XRC) were taken using CuK_α radiation with an angular reproducibility of ±0.0001°. High resolution was achieved with the help of a Ge(220)×4 Bartels monochromator and a 0.05 mm slit installed in front of the detector.

Processing and analysis of experimental diffractometric data (smoothing, fitting, baseline removal, determination of centers of maximum) were performed using the Fityk, OriginPro software packages (OriginLab Corporation) [7].

3. Results and discussion

Fig. 2 shows the X-ray diffraction results for GaN/Si (111) heterostructures. Only two reflections were observed in the 2θ-ω scans. The first one (less intense) was a reflection from (111) plane of the silicon substrate, and the second, (0002), was a reflection from the GaN plane, respectively. No other reflections were detected, indicating that the grown GaN layer was in a monocrystalline state and had a hexagonal lattice with wurtzite structure.

To determine the crystalline quality of the epitaxial films, symmetric and asymmetric X-ray 2θ-ω scans and high-resolution ω rocking curves were obtained for the (0002) and $(10\bar{1}2)$ planes. The results are shown in Fig. 3. It can be seen that the Bragg angle of the maxima of the symmetric and asymmetric reflections in the 2θ-ω scans (Fig. 3a, c) differ between samples A and B, which means that they have different parameters of the crystal lattice of the GaN layer.

Moreover, besides the main high-intensity maxima, the 2θ-ω $(10\bar{1}2)$ scan for sample A (Fig. 3C) has an additional diffraction pattern (in the region of large Bragg angles). There is

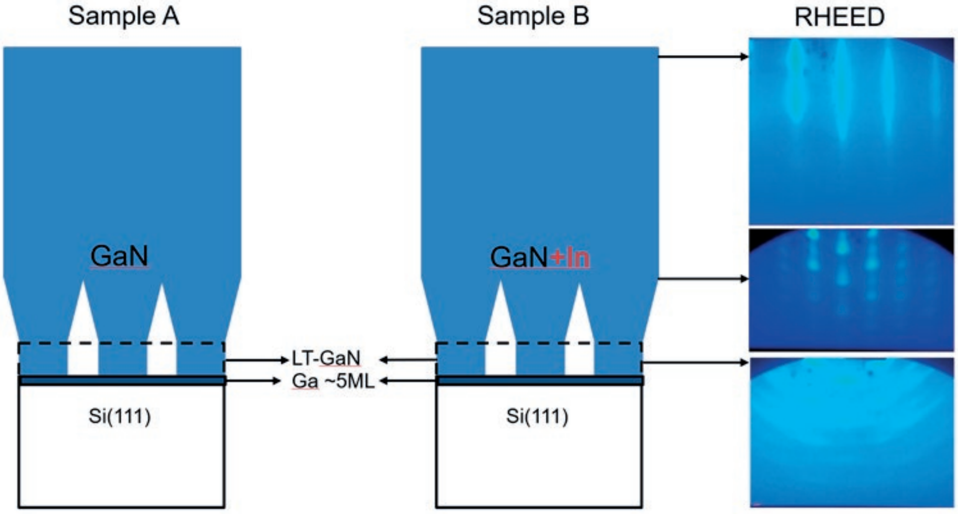

Fig. 1. Schematic representation of samples GaN/Si(111) heterostructures

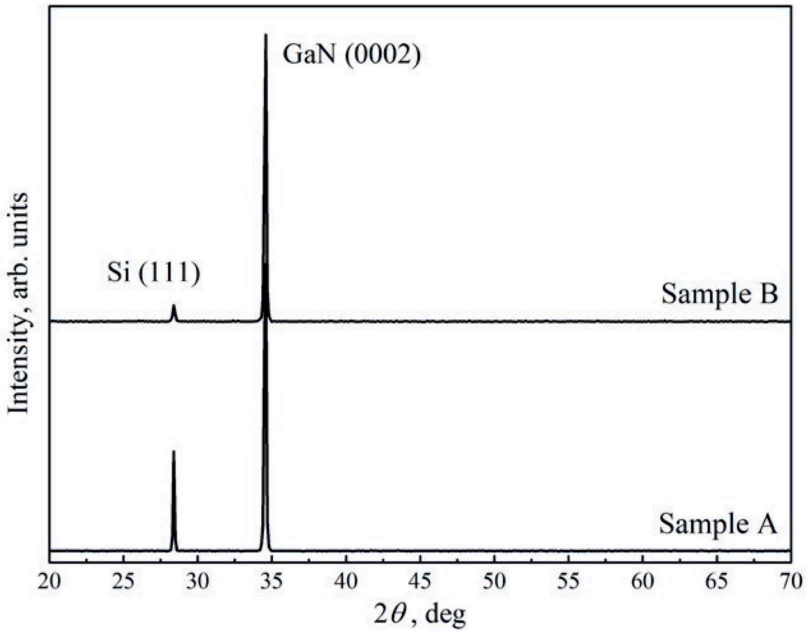

Fig. 2. XRD 2θ-scans for the GaN/Si(111) heterostructures

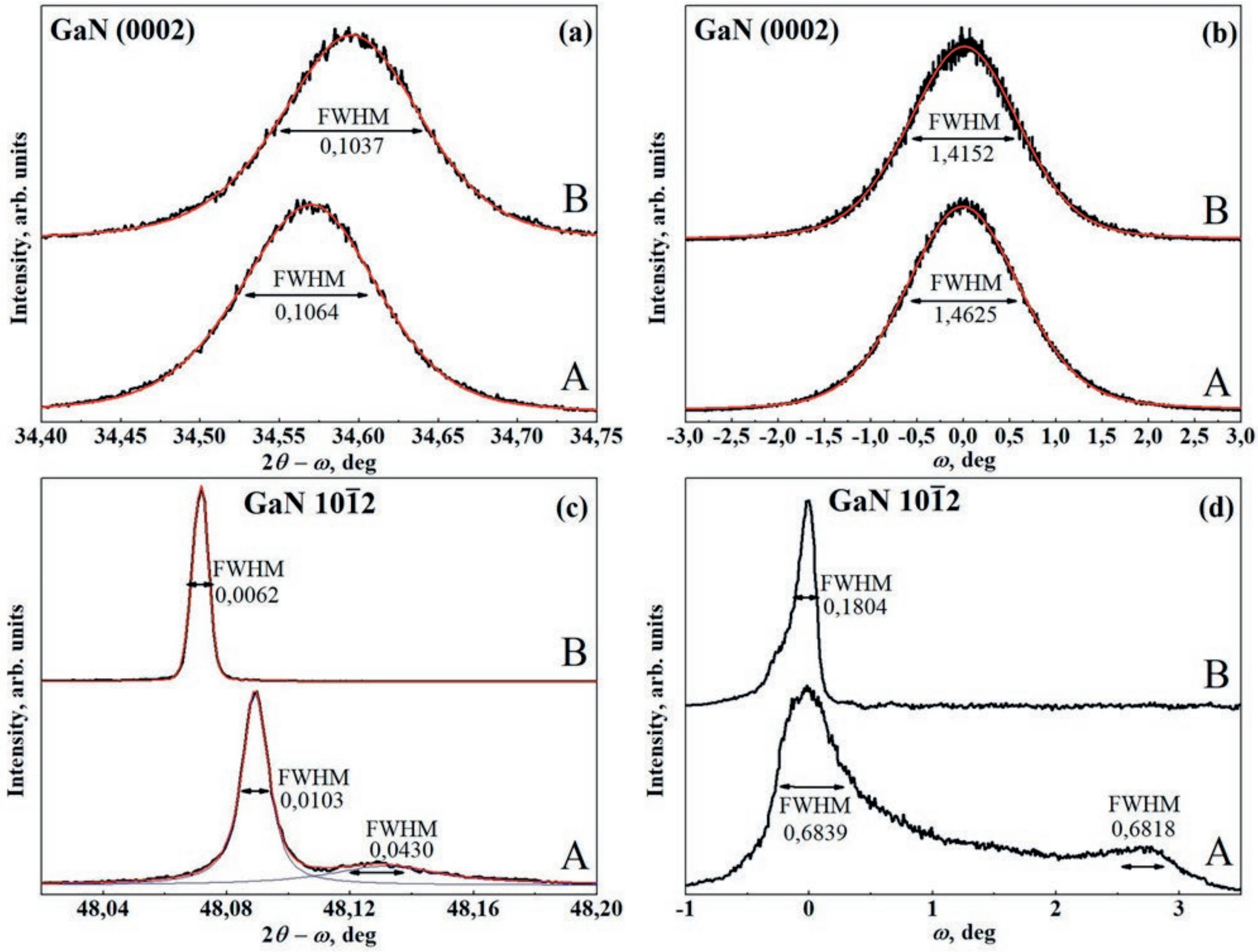

Fig. 3. XRD 2θ-scans (a,c) and ω-swing curves (b,d) GaN/Si(111) simples

also an additional low-intensity maximum at the (10$\bar{1}$2) of the ω rocking curve for sample A (Fig. 3d). These facts may indicate that a sublayer with a smaller lattice parameter than that of the main GaN layer was formed in sample A.

For each diffraction maximum, the full width at half maximum (FWHM) was determined using XRD scans. The analysis of FWHM values provided further information on the crystalline quality of the samples. Thus, the FWHM of the diffraction reflection in the 2θ-ω scan showed the presence of inhomogeneous deformation and changes in the grains size of the sample. Additionally, the FWHM of the maximum in the ω rocking curve provided information on the orientation of the crystallites in the epitaxial layer, i.e. mosaic structure.

The analysis of the obtained results (Fig. 3) revealed that the FWHMs of the main diffraction maximum in the 2θ-ω and ω-scans for the (0002) plane had similar values for samples A and B, while the FWHM of the (10$\bar{1}$2) reflection was lower for sample B. This may also indicate that in the direction of growth of the GaN layer, both samples had the same relaxation values and degrees of mosaic structure, while in the growth plane these values, as well as the lattice parameters, differed between the samples. The measured FWHM (0002) values in the 2θ-ω scans for samples A and B were 360 and 350 arcseconds, respectively. We compared the obtained values with those presented in the study by Jae-Hoon Lee et al. [8] where a high-quality GaN layer (~1.5 μm) with reduced stress and dislocation density was grown on Si substrate. As a result, it can be concluded that the FWHM values for the (0002) plane were similar while the FWHM value for the $(10\bar{1}2)$ plane was much lower. Also, the FWHM values for the (0002) plane on the ω rocking curves were much higher than the FWHM value in the 2θ-ω scans. It means that at the same value of the film's mosaic structure GaN layer should have better relaxation in the growth direction.

Asymmetric X-ray diffraction scans for the $(10\bar{1}2)$ plane provided information for directions coinciding with *a* and *c* axes of the wurtzite lattice [9]. The FWHM value for the $(10\bar{1}2)$ reflection was higher in the ω scans than in the 2θ-ω scans. This indicates at a lower stress due to the lattice mismatch in this direction; however, it also means more pronounced mosaic structure. Moreover, the FWHM value for the $(10\bar{1}2)$ reflection in the ω-scan for sample A was significantly higher than that one for sample B.

It is well known that an increase in the FWHM of X-ray reflections, which is associated with both the orientation and microdeformation of crystallites in the epitaxial layer, represents the formation and changes in the density of screw (c-type) dislocations along *c* crystal axis and edge (a-type) threading dislocations. In [10], it was shown that the values of the density of screw and edge dislocations in the epitaxial layers of nitrides can be estimated by ω rocking curves based on the following relations [11]:

$$D_S = \frac{\beta_{0002}^2}{4.35 b_S^2} \tag{1}$$

$$D_E = \frac{\beta_{10\bar{1}2}^2}{4.35 b_E^2} \tag{2}$$

Here, β_{0002} and $\beta_{10\bar{1}2}$ are the FWHMs for the symmetric and asymmetric omega scans, while $b_S = 5.1864$ Å and $b_E = 3.1890$ Å are the lengths of the Burgers vectors. The calculations showed (see Table 1) that the density of screw dislocations in the epitaxial layer of GaN in both samples was higher than that one of the edge dislocations. However, the density of screw and edge dislocations in sample B was lower than in the sample A.

HRXRD data were used to determine lattice constants *a* and *c* for the epitaxial layer with the wurtzite structure [12].

Experimentally obtained values of the lattice constants were used to determine the relaxation coefficient *R* of GaN layer relative to the Si substrate, the biaxial stress coefficient, and the residual stresses (see Table 1).

The lattice relaxation in the epitaxial layer can be calculated by the formula:

$$R = \frac{a_e - a_S}{a_0 - a_S} \tag{3}$$

where a_e is the lattice parameter measured experimentally; a_S is the lattice parameter equivalent to that one which the layer would take if it was completely deformed; and a_0 is the lattice parameter which the layer would take in the bulk state.

The monocrystalline silicon (substrate) oriented along the (111) direction had the effective lattice parameter $a_S = 3.84$ Å [13]. The values of the lattice parameter for unstressed GaN were taken from previous studies: $c_0 = 5.1864$ Å, $a_0 = 3.1890$ Å [14,15].

The obtained results (Table 1) indicate that GaN layer grown on a Si substrate by the proposed method was almost ~99% strain-free for the samples of both types.

Since the *a* parameter of the GaN wurtzite lattice is larger than the effective lattice parameter of the silicon substrate with (111) orientation, cooling of the sample after its growth is accompanied by appearance of biaxial deformation in the GaN epitaxial layer .[16]. The in-plane biaxial stress σ_{xx} of GaN can be calculated as follows [17–19]:

$$\sigma_{xx} = -M\varepsilon_{xx}. \tag{4}$$

Deformations in the ε_{xx} plane (along the *a-axis*) and in the direction of the ε_{xx} growth (along the *c-axis*) were calculated as follows [20]:

$$\varepsilon_{xx} = \frac{a_e - a_0}{a_0}, \varepsilon_{zz} = \frac{c_e - c_0}{c_0} \tag{5}$$

M is biaxial elastic modulus.

$$M = C_{11} + C_{12} - 2\frac{C_{13}^2}{C_{33}} \tag{6}$$

Table 1. Results of X-ray diffractometry, Raman and PL spectroscopy

Sample	Structure component	Lattice parameter, Å		Dislocation density		Relaxation coefficient, *R*, %	Level of residual biaxial stresses, σ_{xx}, GPa
		c_e	a_e	Screw dislocations, D_S	Edge dislocations, D_E	–	
A	GaN	5.1850	3.1903	$5.1 \cdot 10^{-10}$	$3.1 \cdot 10^{-10}$	99.7 %	0.270
	GaN- bound	5.1850	3.1582	–	–	–	–
	Si	-	5.432	–	–	–	–
B	GaN	5.1813	3,1952	$5.0 \cdot 10^{-10}$	$2.1 \cdot 10^{-9}$	99.0%	0.930
	Si	-	5.427	–	–	–	–

According to (8), for GaN with a wurtzite lattice M ~ 479 ГПа.

The calculations showed (see Table 1) that the level of residual in-plane biaxial stress for sample A was at ~270 MPa, while for sample B it was almost three times higher and attained up to ~930 MPa.

4. Conclusions

The paper describes the structural features of the growth of GaN layers synthesized by PA MBE on silicon substrates without substrate nitridation and without the formation of an intermediate aluminum-containing layer.

High-resolution X-ray diffractometry was used to show that the suggested method can be used to grow strain-free GaN films.

It was found that in GaN layers grown directly on the Si substrate after the passivation of its surface with Ga atoms, the value of residual strain is of 300 MPa, while the use of indium atoms as a surfactant during the growth of the GaN layer results in a higher residual strain.

The obtained results are important for understanding the viability of the proposed approach for the formation of GaN layers directly integrated with Si without substrate nitridation and formation of an aluminum-containing buffer. This method opens up new opportunities for designing AIIIN-based optoelectronic devices.

Contribution of the authors

The authors contributed equally to this article.

Conflict of interests

The authors declare that they have no known competing financial interests or personal relationships that could have influenced the work reported in this paper.

References

1. Li J., Xu Y., Tao J., … Xu K. Study on nucleation and growth mode of GaN on patterned graphene by epitaxial lateral overgrowth. *Crystal Growth & Design*. 2023;23(8): 5541–5547. https://doi.org/10.1021/acs.cgd.3c00171

2. Almalawi D., Lopatin S., Edwards P. R., … Roqan I. S. Simultaneous growth strategy of high-optical-efficiency GaN NWs on a wide range of substrates by pulsed laser deposition. *ACS Omega*. 2023;8(49): 46804–46815. https://doi.org/10.1021/acsomega.3c06302

3. Lim S. H., Bin Dolmanan S., Tong S. W., Liu H. Temperature dependent lattice expansions of epitaxial GaN-on-Si heterostructures characterized by in- and ex-situ X-ray diffraction. *Journal of Alloys and Compounds*. 2021;868: 159181. https://doi.org/10.1016/j.jallcom.2021.159181

4. Seredin P. V., Lenshin A. S., Zolotukhin D. S., Arsentyev I. N., Zhabotinskiy A. V., Nikolaev D. N. Impact of the substrate misorientation and its preliminary etching on the structural and optical properties of integrated GaAs/Si MOCVD heterostructures. *Physica E: Low-dimensional Systems and Nanostructures*. 2018;97: 218–225. https://doi.org/10.1016/j.physe.2017.11.018

5. Seredin P. V., Goloshchapov D. L., Lenshin A. S., Mizerov A. M., Zolotukhin D. S. Influence of por-Si sublayer on the features of heteroepitaxial growth and physical properties of InxGa1-xN/Si(111) heterostructures with nanocolumn morphology of thin film. *Physica E: Low-dimensional Systems and Nanostructures*. 2018;104: 101–110. https://doi.org/10.1016/j.physe.2018.07.024

6. Mizerov A. M., Timoshnev S. N., Sobolev M. S., … Bouravleuv A. D. Features of the initial stage of GaN growth on Si(111) substrates by nitrogen-plasma-assisted molecular-beam epitaxy. *Semiconductors*. 2018;52(12): 1529–1533. https://doi.org/10.1134/S1063782618120175

7. Vasilkova E. I., Pirogov E. V., Sobolev M. S., Ubiyvovk E. V., Mizerov A. M., Seredin P. V. Molecular beam epitaxy of metamorphic buffer for InGaAs/InP photodetectors with high photosensitivity in the range of 2.2-2.6 um. *Condensed Matter and Interphases*. 2023;25(1): 20–26. https://doi.org/10.17308/kcmf.2023.25/10972

8. Seredin P. V., Glotov A. V., Domashevskaya E. P., Arsentyev I. N., Vinokurov D. A., Tarasov I. S. Structural features and surface morphology of AlxGayIn1-x-yAszP1-z/GaAs(1 0 0) heterostructures. *Applied Surface Science*. 2013;267: 181–184. https://doi.org/10.1016/j.apsusc.2012.09.053

9. Lee J.-H., Im K.-S. Growth of high quality GaN on Si (111) substrate by using two-step growth method for vertical power devices application. *Crystals*. 2021;11(3): 234. https://doi.org/10.3390/cryst11030234

10. Zheng C. D., Mo C. L., Fang W. Q., Jiang F. Y. Effect of the conduction type of Si (111) substrates on the performance of GaN MQW LED epitaxial films. *Advanced Materials Research*. 2013;750–752: 1029–1033. https://doi.org/10.4028/www.scientific.net/AMR.750-752.1029

11. Ene V. L., Dinescu D., Djourelov N., ... Andronescu E. Defect structure determination of GaN films in GaN/AlN/Si heterostructures by HR-TEM, XRD, and slow positrons experiments. *Nanomaterials*. 2020;10(2): 197. https://doi.org/10.3390/nano10020197

12. Lee H.-P., Perozek J., Rosario L. D., Bayram C. Investigation of AlGaN/GaN high electron mobility transistor structures on 200-mm silicon (111) substrates employing different buffer layer configurations. *Scientific Reports*. 2016;6(1): 37588. https://doi.org/10.1038/srep37588

13. Xue J. J., Chen D. J., Liu B., ... Zhang J. P. Indium-rich InGaN epitaxial layers grown pseudomorphically on a nano-sculpted InGaN template. *Optics Express*. 2012;20(7): 8093. https://doi.org/10.1364/OE.20.008093

14. Ng T. K., Holguin-Lerma J. A., Kang C. H., ... Ooi B. S. Group-III-nitride and halide-perovskite semiconductor gain media for amplified spontaneous emission and lasing applications. *Journal of Physics D: Applied Physics*. 2021;54(14): 143001. https://doi.org/10.1088/1361-6463/abd65a

15. Morkoç H. *Handbook of nitride semiconductors and devices: materials properties, physics and growth*. 1st ed. Wiley; 2008. https://doi.org/10.1002/9783527628438

16. *Group IV elements, IV-IV and III-V compounds. Part a - lattice properties.* Madelung O., Rössler U., Schulz M. (eds.). Berlin/Heidelberg: Springer-Verlag; 2001; a1–7. https://doi.org/10.1007/b60136

17. Kisielowski C., Krüger J., Ruvimov S., ... Davis R. F. Strain-related phenomena in GaN thin films. *Physical Review B*. 1996;54(24): 17745–17753. https://doi.org/10.1103/PhysRevB.54.17745

18. Harutyunyan V. S., Aivazyan A. P., Weber E. R., Kim Y., Park Y., Subramanya S. G. High-resolution X-ray diffraction strain-stress analysis of GaN/sapphire heterostructures. *Journal of Physics D: Applied Physics*. 2001;34(10A): A35–A39. https://doi.org/10.1088/0022-3727/34/10A/308

19. Seredin P. V., Glotov A. V., Ternovaya V. E., ... Tarasov I. S. Effect of silicon on relaxation of the crystal lattice in MOCVD–hydride $Al_xGa_{1-x}As$:Si/GaAs(100) heterostructures. *Semiconductors*. 2011;45(4): 481–492. https://doi.org/10.1134/S106378261104021X

20. Seredin P. V., Leiste H., Lenshin A. S., Mizerov A. M. Effect of the transition porous silicon layer on the properties of hybrid GaN/SiC/por-Si/Si(1 1 1) heterostructures. *Applied Surface Science*. 2020;508: 145267. https://doi.org/10.1016/j.apsusc.2020.145267

21. Li Z., Jiu L., Gong Y., ... Wang T. Semi-polar (11-22) AlGaN on overgrown GaN on micro-rod templates: simultaneous management of crystal quality improvement and cracking issue. *Applied Physics Letters*. 2017;110(8): 082103. https://doi.org/10.1063/1.4977094

Information about the authors

Pavel V. Seredin, Dr. Sci. (Phys.–Math.), Full Professor, Chair of Department of Solid State Physics and Nanostructures, Voronezh State University (Voronezh, Russian Federation).

https://orcid.org/0000-0002-6724-0063
paul@phys.vsu.ru

Olga K. Kosheleva, postgraduate student, Department of Solid State Physics and Nanostructures, Voronezh State University (Voronezh, Russian Federation).

https://orcid.org/0009-0002-0068-0002
olgak-98@yandex.ru

Dmitry L. Goloshchapov, Cand. Sci. (Phys.–Math.), Assistant Professor, Department of Solid State Physics and Nanostructures, Voronezh State University (Voronezh, Russian Federation).

https://orcid.org/0000-0002-1400-2870
goloshchapov@phys.vsu.ru

Nikita S. Buylov, Cand. Sci. (Phys.–Math.), Educator, Department of Solid State Physics and Nanostructures, Voronezh State University (Voronezh, Russian Federation).

https://orcid.org/0000-0003-1793-4400
buylov@phys.vsu.ru

Yaroslav A. Peshkov, Laboratory Research Assistant, Department of Solid State Physics and Nanostructures, Voronezh State University (Voronezh, Russian Federation).

https://orcid.org/0000-0003-0939-0466
tangar77@mail.ru

Mizerov Andrey Mikhailovich, Cand. Sci. (Phys.–Math.), Leading Researcher, Alferov University, (Saint Petersburg, Russian Federation).

https://orcid.org/0000-0002-9125-6452
andreymizerov@rambler.ru

Sergey N. Timoshnev, Cand. Sci. (Phys.–Math.), Leading Researcher, Alferov University (Saint Petersburg, Russian Federation).

https://orcid.org/0000-0002-9294-3342
timoshnev@mail.ru

Maksim S. Sobolev, Cand. Sci. (Phys.–Math.), Acting Head of the Laboratory of Nanoelectronics, Alferov University (Saint Petersburg, Russian Federation).

https://orcid.org/0000-0001-8629-2064

sobolevsms@gmail.com

Shukrilo Sh. Sharofidinov, Cand. Sci. (Phys.–Math.), Researcher, Ioffe Physical Technical Institute, Russian Academy of Sciences (Saint Petersburg, Russian Federation).

https://orcid.org/0000-0003-0354-5981

shukrillo71@mail.ru

Received 16.10.2024; approved after reviewing 30.10.2024; accepted for publication 15.11.2024; published online 25.06.2025.